



# The superior colliculus encodes gaze commands in retinal coordinates

Eliana M. Klier<sup>1,2,4</sup>, Hongying Wang<sup>1,2,3</sup> and J. Douglas Crawford<sup>1,2,3,4,5</sup>

<sup>1</sup>CIHR Group for Action and Perception, <sup>2</sup>York Centre for Vision Research and Departments of <sup>3</sup>Psychology, <sup>4</sup>Biology and <sup>5</sup>Kinesiology & Health Sciences, York University, 4700 Keele Street, Toronto, Ontario M3J 1P3, Canada

Correspondence should be addressed to J.D.C. ([jdc@yorku.ca](mailto:jdc@yorku.ca))

The superior colliculus (SC) has a topographic map of visual space, but the spatial nature of its output command for orienting gaze shifts remains unclear. Here we show that the SC codes neither desired gaze displacement nor gaze direction in space (as debated previously), but rather, desired gaze direction in retinal coordinates. Electrical micro-stimulation of the SC in two head-free (non-immobilized) monkeys evoked natural-looking, eye-head gaze shifts, with anterior sites producing small, fixed-vector movements and posterior sites producing larger, strongly converging movements. However, when correctly calculated in retinal coordinates, all of these trajectories became 'fixed-vector.' Moreover, our data show that this eye-centered SC command is then further transformed, as a function of eye and head position, by downstream mechanisms into the head- and body-centered commands for coordinated eye-head gaze shifts.

Compared to our understanding of early sensory and late motor codes, the spatial codes used in intermediate sensory-motor transformations remain obscure. Consider the superior colliculus (SC), perhaps the most studied sensorimotor structure in the brain. The SC possesses a multi-layered, topographic map of visual space<sup>1,2</sup> and is a major site for both sensory integration<sup>3</sup> and target selection<sup>4</sup> for the gaze control system (where gaze is the end product of rotations of both the eyes and head). However, the spatial nature of its motor command remains unclear.

Most investigators believe that the SC map codes fixed-vector gaze displacements, independent of initial eye position<sup>5-10</sup>. (We refer to this as the 'gaze-displacement' model.) Nevertheless, there is evidence that stimulation of some posterior SC sites produces position-dependent movements toward a fixed direction in space<sup>11-15</sup>. (We call this the 'gaze-position' model.) This has been interpreted either as a position-dependent artifact of stimulation<sup>16,17</sup> or as evidence for an antero-posterior transition from displacement coding to position coding<sup>12,13</sup>. Either way, this remains a persistent glitch in the popular view that the SC simply encodes fixed-vector gaze displacements.

However, there is a third interpretation that could possibly reconcile the existing data. Several theoretical studies have suggested that the geometry of retinal stimulation and that of gaze displacement, previously assumed to be identical, are indeed significantly different<sup>18,19</sup> (Fig. 1).

When the eye is rotated up or down, purely horizontal points of stimulation on the retina correspond (surprisingly) to targets in space that must be acquired by non-horizontal gaze shifts (Fig. 1). This geometry, a consequence of projecting light onto the interior surface of a rotating sphere, has an important implication for gaze control: any one given retinal representation must be mapped onto many different displacements of gaze, depending on the eye's initial orientation in space. Our previous behavioral studies have shown that the brain correctly accounts for this position-dependent geometry<sup>19-21</sup>, but the underlying neurophysiological mechanism could not be determined.

So how does the SC encode gaze commands? Does it code fixed gaze displacements, desired gaze positions or something else entirely? To answer these questions, we compared theoretical simulations with the trajectories of gaze shifts evoked by electrically micro-stimulating the SC in the head-free monkey. In contrast to single-neuron recording, which provides data related to the neural inputs to individual SC cells, electrical micro-stimulation can potentially reveal the motor output of local cell populations in the SC. Stimulation should activate a focal region of the SC map—preferentially recruiting large-axon output neurons—and thus simulate a fixed SC output command. Stimuli were delivered during untrained, head-free gaze fixations (in both dark and dim light) to obtain the necessary range of initial eye and head positions and to promote a background state that was as natural as possible. Several previous studies<sup>5,15,22</sup> have examined SC stimulus-evoked, head-free gaze shifts, but this is the first to record three-dimensional orientations of both the eye and head.

## RESULTS

### Simulations

To illustrate the differences between three possible models of visual-motor representation, we simulated gaze shifts that would be evoked by activating three fixed points on the SC map (Fig. 2). The type of gaze shifts evoked and their dependence on initial gaze position was determined by the nature of the signal that the SC sent to the saccade generator<sup>18</sup> (see Methods). In the case of the gaze-displacement model (Fig. 2a-c), three fixed-movement vectors (30°, 60° or 90° left) were input to the saccade generator. Thus, the resultant gaze trajectories followed parallel displacement paths, independent of initial gaze position or the size of the movement. In contrast, with the gaze-position model (Fig. 2d-f), three desired gaze-in-space positions (30°, 60° or 90° left) were input to the saccade generator. Thus, for a given SC site, the gaze paths converged toward a single point in space. Much of the research in this field has focused on the distinction between these two models<sup>5-15</sup>.

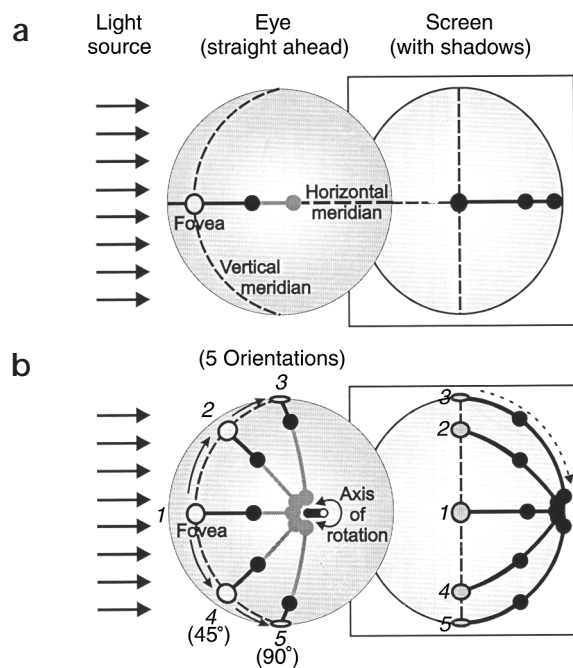


**Fig. 1.** Position-dependent geometry of retinal projection and gaze displacement. A semi-transparent 'eye' is viewed from a behind-right perspective, and the eye is backlit so that the shadows project onto a frontal screen. This projection system is not arbitrary; it mirrors the geometry of the raw two-dimensional eye-coil signals used to measure gaze in physiological studies. **(a)** View of eye looking straight ahead, with the fovea (open disk) oriented at the back of the eye. We define the horizontal meridian of the retina as the dashed equatorial line at this position. Two sites of retinal stimulation (black and gray circles) are represented as 'retinal error' vectors emanating rightward from the fovea; one 40° right (black line) and one 80° right (gray line). These correspond to 40° and 80° rightward visual targets (dispensing with the optical inversion), as shown by the shadows projected on the screen (black circles). This is the trivial situation in which a point of horizontal stimulation on the retina calls for a purely horizontal eye movement to acquire the target. **(b)** Five different static eye orientations (1–5), accounting for the possibility of the eye rotating up or down about its horizontal axis by 45° or 90°. The stimulus vectors remain fixed anatomically on the same horizontal retinal meridian (so that from our space-fixed perspective, they now seem rotated to non-horizontal lines). Horizontal displacements (in retinal coordinates) now correspond to non-horizontal displacement vectors in visual space (screen, right): the vectors become more and more oblique as a function of the length of retinal vector and the amount of eye rotation. For example, at position 3, the 80° rightward retinal target would call for an eye movement qualitatively like the one indicated by the dashed arrow on the screen.

Finally, we simulated the expected results of activating sites that code fixed movement vectors in retinal coordinates, that is, a retinal model (Fig. 2g–i). In simulating this model, fixed retinal errors were output from the SC and the required position dependencies were incorporated downstream<sup>18,19</sup>. One can expect that a fixed retinal error should result in a surprisingly complex, position-dependent pattern of motion (Fig. 1). As predicted, the retinal model produced small, fixed-vector-like gaze shifts that converged minimally for small retinal errors (Fig. 2g), and produced larger, more convergent movements for increasingly larger retinal errors (Fig. 2h and i). Again, these converging movements are not mistakes, but rather, represent the correct trajectories required to satisfy fixed retinal inputs<sup>18,19</sup>.

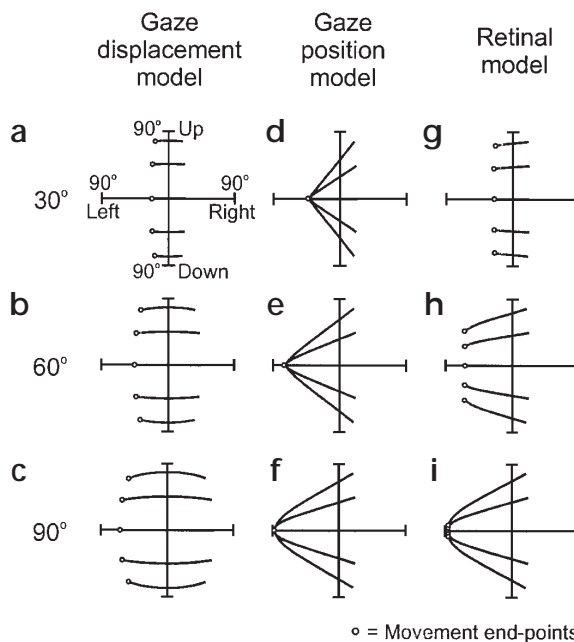
### Stimulus-evoked gaze shifts

To test these models, we analyzed gaze shifts evoked by micro-stimulating 77 SC sites (of which 55 met our criteria for quantitative analysis; see Methods) in two head-free monkeys. As expected (Fig. 3), SC stimulation evoked primarily contralateral gaze shifts, in this case, to the left. Also, as found in previous studies<sup>7–15</sup>, stimulations evoked small gaze shifts for anterior SC sites (Fig. 3a) and progressively larger movements as the stimulations were delivered more posteriorly (Fig. 3b and c). Most of these gaze shifts—even the smaller ones—were associated with a combination of both eye (Fig. 3d–f) and head (Fig. 3g–i) movements. Thus, our study was consistent with others that suggest that the SC encodes

gaze<sup>12,13,22–25</sup>, with individual eye and head contributions coordinated downstream. However, which of the three models described above (Fig. 2) best represents the coding of the SC?

To address this question, we first looked at the overall pattern of evoked gaze shifts. The smaller stimulus-evoked gaze shifts (Fig. 3a) seemed to be roughly fixed in both length and direction. In contrast, as the stimulations were applied more posteriorly (Fig. 3b and c), a more convergent pattern of movements emerged. For the most posterior sites (Fig. 3c), it appeared that these movements were converging toward a specific direction in space coordinates. Thus, small gaze shifts appeared to conform to the gaze-displacement model, whereas larger ones were more consistent with the gaze-position model. However, interpreted in light of our simulations (Fig. 2), the overall pattern of move-

**Fig. 2.** Simulated gaze shifts produced by three models of gaze coding in the SC. Gaze is represented as the tip of a unit vector parallel to the visual axis and projected from behind onto the frontal plane. Fixed-axis rotations produce slightly curved trajectories in these projections. **(a–c)** The gaze-displacement model. Gaze trajectories (O—) were set to follow fixed gaze displacements. Initial gaze positions are either 15°, 30° or 45° right and either 0°, ±30° and ±60° vertical. **(d–f)** The gaze-position model. Desired gaze-in-space was input to the gaze generator. **(g–i)** The retinal model. Gaze paths move according to fixed retinal errors. Initial gaze positions for both the spatial and retinal models are 15° right and either 0°, ±30° and ±60° vertical.



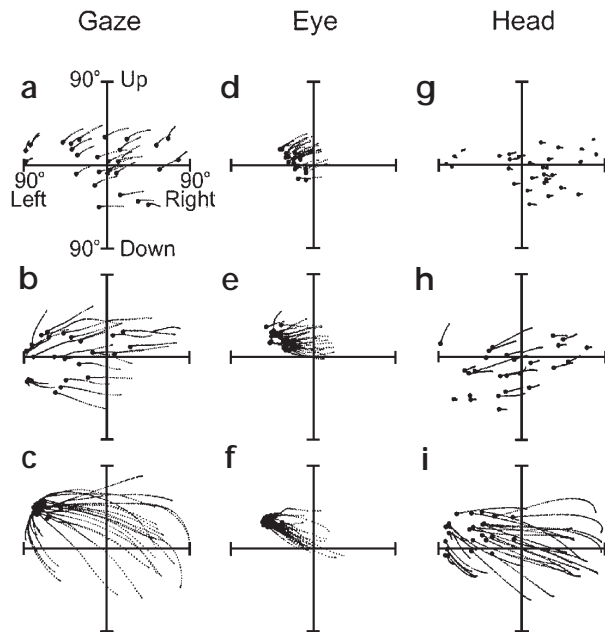


**Fig. 3.** Trajectories evoked by stimulating three SC sites. Gaze (a–c), eye (d–f) and head (g–i) plots are shown for a relatively anterior site (~30° gaze shifts; top row), an intermediate site (~60° gaze shifts; middle row) and an extremely posterior site (~90° gaze shifts; bottom row). Data is plotted in space coordinates and the final endpoints of each movement are shown (black circles). Eye trajectories were plotted up until the end of the gaze shift portion of the movement, whereas head trajectories were plotted until the head movement stopped.

ment seemed to most closely follow the predictions of the retinal model (Fig. 2g–i).

To test this directly, we used initial three-dimensional eye orientations to convert our gaze trajectories into retinal coordinates (that is, a coordinate system based on the three-dimensional orientation of the eye at the beginning of the stimulus-evoked gaze shift). This involved rotating instantaneous gaze positions (at each point along the entire gaze trajectory) by the inverse of the initial eye orientation in space (see Methods). Figuratively speaking, this process takes the resultant gaze trajectories in space (screen view in Fig. 1) and projects them back onto the retina (eye view in Fig. 1) in order to determine the pattern of retinal stimulation that caused these movements. If the retinal model is correct, then all of our data should become fixed-vector in this new coordinate system.

The mathematically correct transformation does not merely shift the gaze trajectories so that their tails align with the center, but instead results in a qualitatively different pattern of movements (Fig. 4). Despite the large variety of gaze trajectories in space coordinates, some fixed-vector (Fig. 4a) and others converging (Fig. 4b and c), the movements evoked from a given SC site essentially superimpose in retinal coordinates (Fig. 4d–i). In other words, all three of these SC sites produced fixed gaze shifts in retinal coordinates, typical of all our data.

To quantify these observations across a wider data set, we calculated a 'convergence index' for each stimulation site (see Meth-

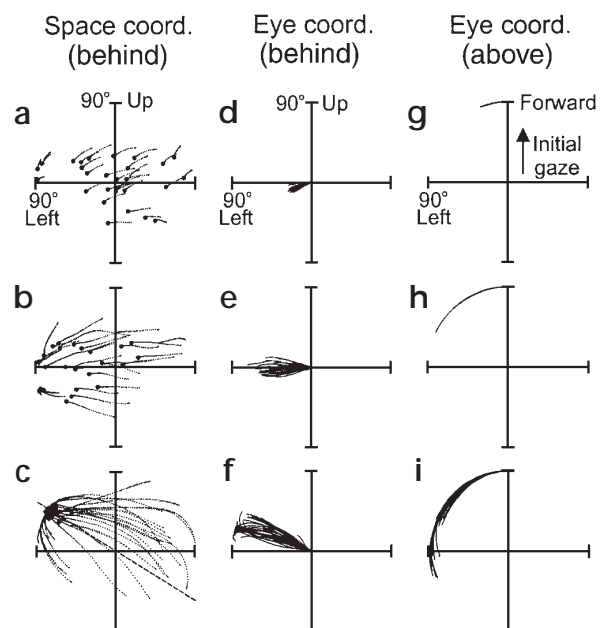
ods). In brief, we computed the characteristic direction of gaze displacement across the center position (for example, Fig. 4c, dashed line) and then plotted gaze displacement as a function of initial gaze direction along the orthogonal axis. The latter step was necessary because the characteristic gaze displacement was not generally purely horizontal, but also had various site-specific vertical components. The slope of the resultant line (orthogonal displacement as a function of orthogonal initial position) was then used as our convergence index.

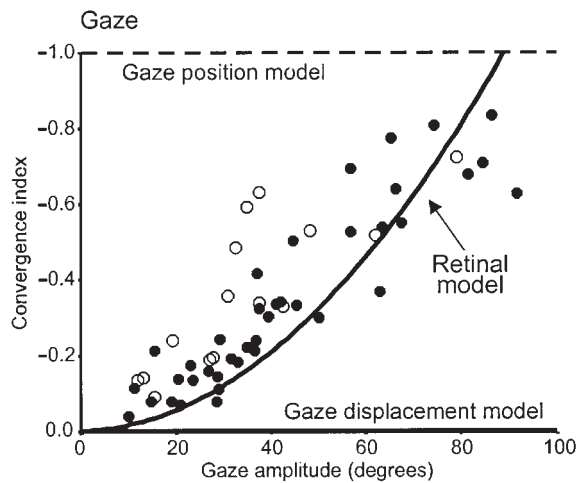
The important test was to plot the convergence indices for all the sites as a function of each site's characteristic gaze magnitude (Fig. 5). Here, each model predicts a different curve. The data in the 0°–30° range along the abscissa (examined in most of the previous primate electrophysiological studies<sup>5–10</sup>) agreed fairly well with the gaze-displacement model. In contrast, the data at the top end of the range (similar to movements evoked in some head-free studies<sup>11–15</sup>) agreed better with the gaze-position model. However, when the full range of data was considered, it became clear that the overall pattern was best described by the predictions of the retinal model.

#### Eye-head coordination

The main result of our study—that the SC motor code uses a simple retinal geometry—has implications for downstream motor transformations. How, then, are retinally fixed SC codes (for example, Fig. 4f) mapped onto the very different position-dependent gaze trajectories observed in space coordinates (for example, Fig. 4c), particularly for more posterior SC sites? Our SC data cannot reveal the neural mechanisms for these reference

**Fig. 4.** Gaze in retinal coordinates. (a–c) Gaze trajectories in space coordinates (view from behind, as in Fig. 3). (d–f) Gaze in retinal coordinates, view from behind. At the origin, one is looking down the initial gaze line from behind the fovea. Each movement begins at the origin and proceeds in a direction and distance proportional to the gaze shift. Subtle variations in gaze displacement direction in retinal coordinates may be accounted for as minor changes in the underlying neural state superimposed on the stimulus-evoked activity. (g–i) Gaze in retinal coordinates, view from above. Each point along the gaze trajectory represents the tip of a vector projecting from the origin. The eye's initial pointing direction is aligned with the positive y-axis (arrow) and each leftward movement proceeds in a counterclockwise direction. Differences in the amplitude of some trajectories is due to an inverse relationship with initial eye and head positions.





frame transformations, but they can help show how SC gaze commands are partitioned into coordinated movements of the eyes and head (Fig. 6).

In contrast to gaze (Fig. 5), the convergence index for the eye-in-head (Fig. 6a) initially rose steeply as a function of gaze amplitude, but then reached a plateau (near 100%) at  $\sim 70^\circ$  gaze displacement. There was close agreement between the curves of best fit for the two monkeys (Fig. 6a). A temporal analysis of the off-axis components of these highly convergent eye-in-head movements revealed time constants that were in the normal saccade range<sup>16</sup> (for example, mean  $\pm$  s.e.m.,  $24.66 \pm 1.12$  ms, at the site with the largest convergence index). After comparing these data to previous investigations, it is apparent why gaze seems to converge more strongly when the SC is stimulated with the head fixed<sup>11–14</sup> (that is, where the gaze shift is identical to the evoked eye saccade).

In our data, the head also made a significant contribution toward the gaze shifts. In comparison with the eye plot, the head convergence index (Fig. 6b) began to rise later (that is, for gaze shifts greater than or equal to  $10^\circ$ ) and grew more gradually. However, the head's convergence index continued to increase where the convergence index of the eye leveled off. Thus, for smaller gaze shifts, the eye provided the greatest contribution to the overall gaze convergence index, but for larger gaze shifts, the head made a progressively larger contribution, much like the relative contributions of the eye and head for gaze shifts in a single dimension<sup>26</sup>.

#### DISCUSSION

This study suggests two important and inseparable conclusions. First, that the SC codes gaze commands as displacements in a retinal frame, and second, that downstream structures must then perform the reference frame transformation required to map this code onto accurate gaze displacement commands. In retrospect, this retinal interpretation is consistent with the predominance of retinal inputs to the SC<sup>27,28</sup>, the retinotopic topography of this structure<sup>1,2,27,28</sup> and previous suggestions that the SC uses a visual code

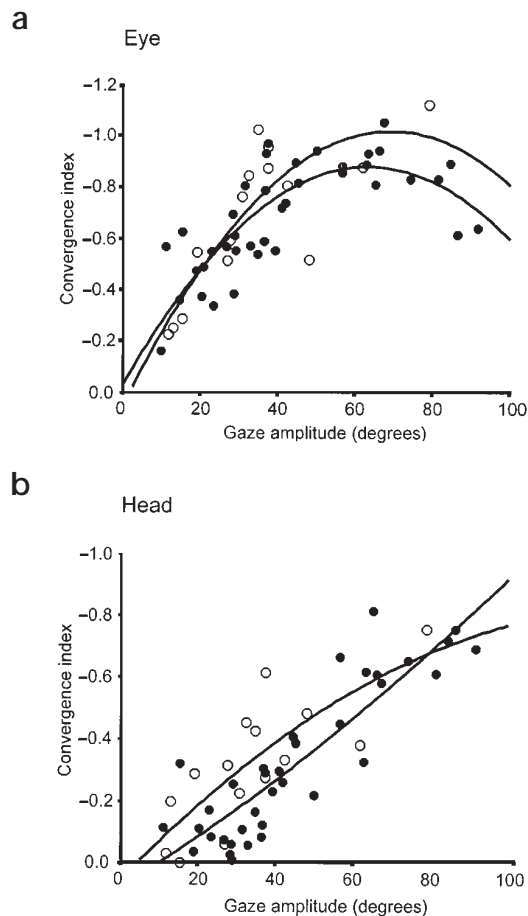
**Fig. 6.** Separate convergence indices for stimulus-evoked eye and head movements. (a) Convergence index for the eye-in-head at the end of the gaze shift/saccade. (b) Convergence index for the head at end of head movement associated with gaze shift. All are plotted as function of characteristic gaze amplitude calculated from gaze data. Best-fit lines are shown for each of the two monkeys (white circles, black circles). Indices calculated for the eye-at-end-of-head-movement and head-at-end-of-eye-movement were slightly different but followed the same pattern reported here.

**Fig. 5.** A convergence index determines the most suitable model of SC coding. Gaze convergence indices from two monkeys (first monkey, white circles; second monkey, black circles) are plotted against the characteristic gaze amplitude for each stimulation site. The gaze-displacement model predicts a fixed convergence index of 0 (slope along the abscissa), whereas the gaze-position model predicts a fixed convergence index of  $-1$  (dashed line). The retinal model requires that convergence indices be small for small gaze amplitudes, but then increase non-linearly for larger gaze amplitudes (solid line). The data favor the retinal model and indeed followed its predictions very closely. The only discernable difference from the retinal model curve was that the line of actual data tended to be slightly more linear (perhaps because the brain is using a linear approximation within this transformation).

upstream from position-dependent saccade commands<sup>29,30</sup>.

This study also illustrates the importance of accounting for the three-dimensional geometry of gaze control (Fig. 1) when interpreting gaze signals. Consider how one might have interpreted the same data without the retinal model (that is, with only the gaze-displacement and gaze-position models for guidance). From such a perspective, Fig. 5 might be taken to suggest a gradual transition from gaze-displacement coding to gaze-position coding as one moves posteriorly through the SC. However, this is not an attractive option, because it would require two different gaze control systems downstream from the SC.

Perhaps a more attractive interpretation (if one had to choose between the two classical models) would be to choose the gaze-displacement model and then propose the following: first, that the position-dependent convergence factor is produced by some





mechanism downstream, second, that there is usually a physiological mechanism that corrects for this factor, and third, that stimulating the SC fails to evoke this mechanism<sup>16,17</sup>. There is indeed evidence that SC stimulation fails to evoke a mechanism for adaptation and position compensation of saccade amplitude<sup>30</sup>. This could account for the position dependence of gaze amplitudes in saccades evoked by SC stimulation<sup>11–15</sup>. It is also likely that some of our largest gaze shifts were truncated (Fig. 4i) because the head was near its mechanical limit and the body was restrained. However, there is no such evidence for a mechanical effect of the kind required to explain the consistent directional effects shown in this study. Indeed, as reviewed elsewhere<sup>18</sup>, it is highly unlikely that the eye (or head) has the mechanical position dependencies required to explain these large, actively generated, off-axis saccade components.

With the retinal model in hand, there is no need to contrive such arguments. The retinal model fits the entire data range and explains its specific and necessary role in the visual–motor transformation. As our previous theoretical analysis shows, if there is a position-dependent convergence factor downstream from the colliculus—whether neural or mechanical—it is not a mistake to be undone, but rather a vital component of the reference frame transformation for gaze shifts<sup>18,31</sup>.

This brings us back to the second major conclusion of this study, that the position-dependent transformation must be located downstream from the SC and involves the coordinated contributions of both the eye and head. This transformation is inherently non-linear because it requires that oculocentric visual signals be mapped, not only onto ‘same-direction’ gaze vectors in a motor frame, but also onto orthogonal movement components as a function of the orthogonal gaze position component.

How then, would this be done? Again, it is unlikely that mechanical factors alone can account for this transformation<sup>18</sup>. A more likely neural mechanism was identified in our previous model simulation, in which a three-layer network learned to map retinal visual commands onto the correct motor vectors for saccades<sup>31</sup>. Our analysis revealed that the network accomplished this by using a ‘cascade’ of vectorial movement commands, simply modulating these by orthogonal eye position signals so that they ended up pointing in the right direction. This theoretical result awaits experimental confirmation, but seems to be an economical solution to the kind of transformation that the brainstem would need to perform on its SC inputs.

The reference frame transformation discussed here pertains to visual–motor execution and should not be confused with eye-to-head reference frame transformations that have been proposed to update internal maps of spatial target locations<sup>32,33</sup>. Indeed, such maps are not found downstream from the SC and (on the whole) are quite rare elsewhere in the brain. An alternative mechanism for spatial updating that is consistent with the current results would be to update within retinocentric maps to compensate for eye movements, thus keeping them in register with actual visual space. Signals consistent with such a mechanism have been observed in several visual–motor areas<sup>34,35</sup>, including the SC<sup>36</sup>. However, of the various spatial representations held in these maps, only those selected for action would have to be put through the downstream reference frame transformations discussed in this paper<sup>37–39</sup>.

The current study adds to a growing body of evidence that the on-line representation of visual–motor space takes the form of a ‘virtual map’<sup>34–36</sup>. Although subjective intuition may tell us that we possess an on-line map of absolute visual space, the current experiment shows that, at least in the orienting system, the geometry of the retina persists right down to the level of motor

coding in the brainstem SC. Coupled with the ‘vectorial cascade’ model discussed above<sup>31</sup>, these factors obviate the need for higher-level, multi-representational maps for on-line visual–motor control. Such a scheme provides for a highly economical mapping of space, while allowing for seamlessly accurate interaction with the external world.

## METHODS

Two monkeys (*Macaca fascicularis*) were surgically prepared for three-dimensional eye and head movement recordings as described previously<sup>40</sup>. These protocols were in accordance with Canadian Council on Animal Care guidelines and were pre-approved by the York University Animal Care Committee. Each monkey wore a primate jacket and sat in a modified Crist Instruments primate chair such that its head and neck were free to move as desired. The upper body (to the shoulders) was prevented from rotating in the yaw direction (that is, movement around an earth-vertical axis) by the use of plastic molding and restraints that attached the primate jacket to the chair.

After recording from midbrain burst-tonic neurons (in the interstitial nucleus of Cajal) to set an anatomic reference point, the SC was identified by recording neural activity from bilateral SC sites in the head-fixed monkeys. If burst activity was heard along with corresponding, contralateral eye movements, then the site was deemed to be a potential SC site. Potential SC sites were further confirmed by observing eye movements elicited after head-fixed stimulations (data not shown). Later, the sites were marked and the brains removed for histological confirmation.

Monkeys could move their eyes and heads freely and naturally, and were encouraged to use their entire motor ranges through the presentation of novel visual objects (in dim light) and novel sounds (in the dark). Stimulations with pulse trains (50  $\mu$ A, 500 Hz) of 200 ms<sup>22</sup> were then delivered to SC sites on both sides of the midline, in dim light and in the dark. (Data from both conditions showed qualitatively similar results; however, this paper only shows data from the dim light condition because the initial position range was larger.) The resultant eye and head movements were recorded at 500 Hz for further analysis<sup>40</sup>.

**Simulations.** Simulated saccade trajectories and theoretical convergence indices were computed with the use of a previously published model<sup>18</sup>. This model generates accurate, kinematically correct saccades using a transition from a retinal gaze command, to a desired gaze–position command, to a desired gaze–displacement command (upstream from a realistic saccade generator and eye muscles). The three possible models, in which the SC could encode gaze, were simulated by inputting a fixed motor command at each one of these three levels (one at a time) and then allowing the initial gaze position to vary. The initial gaze positions used in the simulations were chosen to match the range of initial eye positions seen in our data.

**Computing gaze in retinal coordinates.** Three-dimensional initial eye positions were used to compute gaze directions in retinal coordinates ( $G_{\text{eye}}$ ) by the following formula:

$$G_{\text{eye}} = q^{-1} G_{\text{space}} q$$

Here,  $q$  is the initial eye-in-space quaternion at the beginning of each movement (that is, when the stimulus was delivered),  $q^{-1}$  is its inverse,  $G_{\text{space}}$  describes instantaneous two-dimensional gaze direction, and the operation between the variables is quaternion multiplication<sup>18</sup>.

In retinal coordinates (Fig. 4d–i),  $G_{\text{eye}}$  is represented by a unit vector emanating from the fovea through the center of rotation of the eye. The above formula was first applied to the initial  $G_{\text{space}}$ , which represents where the eye was looking when the stimulus was delivered. The formula was then applied to each instantaneous gaze vector along the entire gaze trajectory to generate eye-centered trajectories (like in Fig. 4d–i).

**Convergence index.** The convergence index for each stimulation site was computed in the following manner. First, a multiple linear regression analysis was performed on the stimulus-induced displacement of gaze



as a function of initial gaze position. In this way, a 'characteristic gaze vector' was computed that describes the theoretical gaze trajectory that would be elicited if the eyes and head were initially pointing straight ahead. (This vector took into account between 30 and 60 stimulations per site.) Second, all the stimulus-induced gaze trajectories were then rotated into a new coordinate system where the characteristic gaze vector acted as the new abscissa. Third, from this new coordinate system, we plotted graphs of off-axis gaze magnitude versus off-axis initial gaze position (off-axis meaning the component orthogonal to the characteristic gaze vector). Finally, lines of best fit were computed for these data, and their slopes defined the amount of convergence at each site. Fifty-five of 77 sites tested qualified to be included in this paper on the basis of the following two criteria: first, gaze shifts were consistently evoked during all stimuli, and second, movements of both the eye and head were evoked. In practice, these two factors were associated. Rejected sites tended to lie on the fringes and more superficial sites of the SC.

## ACKNOWLEDGEMENTS

The authors thank D.E. Angelaki, D. Guitton, E.G. Freedman, L.R. Harris, L.E. Sergio and T. Vilis for their comments on the manuscript. E.M. Klier is supported by Canadian N.S.E.R.C. and O.G.S. scholarships. J.D. Crawford is supported by a Canada Research Chair and a Canadian Institute of Health Research (CIHR) grant.

RECEIVED 23 MARCH; ACCEPTED 23 APRIL 2001

1. Schiller, P. H. & Koerner, R. Discharge characteristics of single units in the superior colliculus of the alert rhesus monkey. *J. Neurophysiol.* **34**, 920–936 (1971).
2. Wurtz, R. H. & Goldberg, M. E. Superior colliculus cell responses related to eye movements in awake monkeys. *Science* **171**, 82–84 (1971).
3. Wallace, M. T., Wilkinson, L. K. & Stein, B. E. Representation and integration of multiple sensory inputs in primate superior colliculus. *J. Neurophysiol.* **76**, 1246–1266 (1996).
4. Horowitz, G. D. & Newsome, W. T. Separate signals for target selection and movement specification in the superior colliculus. *Science* **284**, 1158–1161 (1999).
5. van Opstal, A. J., Hepp, K., Hess, B. J., Straumann, D. & Henn, V. Two- rather than three-dimensional representation of saccades in monkey superior colliculus. *Science* **252**, 1313–1315 (1991).
6. Hepp, K., Van Opstal, A. J., Straumann, D., Hess, B. J. M. & Henn, V. Monkey superior colliculus represents rapid eye movements in a two-dimensional motor map. *J. Neurophysiol.* **69**, 965–979 (1993).
7. Robinson, D. A. Eye movements evoked by collicular stimulation in the alert monkey. *Vision Res.* **12**, 1795–1808 (1972).
8. Schiller, P. H. & Stryker, M. Single-unit recording and stimulation in superior colliculus of the alert rhesus monkey. *J. Neurophysiol.* **35**, 915–924 (1972).
9. Stein, B. E., Goldberg, S. J. & Clamann, H. P. The control of eye movements by the superior colliculus in the alert cat. *Brain Res.* **118**, 469–474 (1976).
10. Harris, L. R. The superior colliculus and movements of the head and eyes in cats. *J. Physiol. (Lond.)* **300**, 367–391 (1980).
11. Straschill, M. & Rieger, P. Eye movements evoked by focal stimulation of the cat's superior colliculus. *Brain Res.* **59**, 211–227 (1973).
12. Guitton, D., Crommelinck, M. & Roucoux, A. Stimulation of the superior colliculus in the alert cat. I. Eye movements and neck EMG activity evoked when the head is restrained. *Exp. Brain Res.* **39**, 63–73 (1980).
13. Roucoux, A., Guitton, D. & Crommelinck, M. Stimulation of the superior colliculus in the alert cat. II. Eye and head movements evoked when the head is unrestrained. *Exp. Brain Res.* **39**, 75–85 (1980).
14. McIlwain, J. T. Effects of eye position on saccades evoked electrically from superior colliculus of alert cats. *J. Neurophysiol.* **55**, 97–112 (1986).
15. Paré, M., Crommelinck, M. & Guitton, D. Gaze shifts evoked by stimulation

of the superior colliculus in the head-free cat conform to the motor map but also depend on stimulus strength and fixation activity. *Exp. Brain Res.* **101**, 123–139 (1994).

16. Moschovakis, A. K., Dalezios, Y., Petit, J. & Grantyn, A. A. New mechanism that accounts for position sensitivity of saccades evoked in response to stimulation of superior colliculus. *J. Neurophysiol.* **80**, 3373–3379 (1998).
17. Segraves, M. A. & Goldberg, M. E. in *The Head-Neck Sensory Motor System* (eds. Berthoz, A., Graf, W. and Vidal, P. P.) 292–295 (Oxford Univ. Press, New York, 1992).
18. Crawford, J. D. & Guitton, D. Visual-motor transformations required for accurate and kinematically correct saccades. *J. Neurophysiol.* **78**, 1447–1467 (1997).
19. Klier, E. M. & Crawford, J. D. Human oculomotor system accounts for 3-D eye orientation in the visual-motor transformation for saccades. *J. Neurophysiol.* **80**, 2274–2294 (1998).
20. Crawford, J. D., Henriques, D. Y. P. & Vilis, T. Curvature of visual space under vertical eye rotation: implications for spatial vision and visuomotor control. *J. Neurosci.* **20**, 2360–2368 (2000).
21. Henriques, D. Y. P. & Crawford, J. D. Testing the tree-dimensional reference frame transformation for express and memory-guided saccades. *Neurocomputing* (in press).
22. Freedman, E. G., Stanford, T. R. & Sparks, D. L. Combined eye-head gaze shifts produced by electrical stimulation of the superior colliculus. *J. Neurophysiol.* **76**, 927–952 (1996).
23. Freedman, E. G. & Sparks, D. L. Activity of cells in the deeper layers of the superior colliculus of the rhesus monkey: evidence for a gaze displacement command. *J. Neurophysiol.* **78**, 1669–1690 (1997).
24. Freedman, E. G. & Sparks, D. L. Eye-head coordination during head-unrestrained gaze shifts in rhesus monkeys. *J. Neurophysiol.* **77**, 2328–2348 (1997).
25. Munoz, D. P. & Guitton, D. Control of orienting gaze shifts by the tectoreticulospinal system in the head-free cat. II. Sustained discharges during motor preparation and fixation. *J. Neurophysiol.* **66**, 1624–1641 (1991).
26. Uemura, T., Arai, Y. & Shimazaki, C. Eye-head coordination during lateral gaze in normal subjects. *Acta Otolaryngol.* **90**, 191–198 (1980).
27. Apter, J. T. Projection of the retina on superior colliculus of cats. *J. Neurophysiol.* **8**, 123–134 (1945).
28. Cynader, M. & Berman, N. Receptive field organization of monkey superior colliculus. *J. Neurophysiol.* **35**, 187–201 (1972).
29. White, J. M., Sparks, D. L. & Stanford, T. R. Saccades to remembered target locations: an analysis of systematic and variable errors. *Vision Res.* **34**, 79–92 (1994).
30. Goldberg, M. E. & Bruce, C. J. Primate frontal eye fields. III. Maintenance of a spatially accurate saccade signal. *J. Neurophysiol.* **64**, 489–508 (1990).
31. Smith, M. A. & Crawford, J. D. Self-organizing task modules and explicit coordinate systems in a neural network model for 3-D saccades. *J. Comp. Neurol.* **10**, 127–150 (2001).
32. Andersen, R. A., Essick, G. K. & Siegel, R. M. Encoding of spatial location by posterior parietal neurons. *Science* **230**, 456–458 (1985).
33. Snyder, L. H., Grieve, K. L., Brotchie, P. & Andersen, R. A. Separate body- and world-referenced representations of visual space in parietal cortex. *Nature* **394**, 887–891 (1998).
34. Duhamel, J.-R., Colby, C. L. & Goldberg, M. E. The updating of the representation of visual space in parietal cortex by intended eye movements. *Science* **255**, 90–92 (1991).
35. Russo, G. S. & Bruce, C. J. Neurons in the supplementary eye field of rhesus monkeys code visual targets and saccadic eye movements in an oculocentric coordinate system. *J. Neurophysiol.* **76**, 825–848 (1996).
36. Walker, M. F., Fitzgibbon, J. & Goldberg, M. E. Neurons of the monkey superior colliculus predict the visual result of impeding saccadic eye movements. *J. Neurophysiol.* **73**, 1988–2003 (1995).
37. Henriques, D. Y. P., Klier, E. M., Smith, M. A., Lowy, D. & Crawford, J. D. Gaze-centered remapping of remembered visual space in an open-loop pointing task. *J. Neurosci.* **18**, 1583–1594 (1998).
38. Batista, A. P., Buneo, C. A., Snyder, L. H. & Andersen, R. A. Reach plans in eye-centered coordinates. *Science* **285**, 257–260 (1999).
39. Colby, C. L. & Goldberg, M. E. Space and attention in parietal cortex. *Annu. Rev. Neurosci.* **22**, 319–349 (1999).
40. Crawford, J. D., Ceylan, M. Z., Klier, E. M. & Guitton, D. Three-dimensional eye-head coordination during gaze saccades in the primate. *J. Neurophysiol.* **81**, 1760–1782 (1999).